

## A LOW-REYNOLDS-NUMBER TWO-EQUATION TURBULENCE MODEL FOR PREDICTING HEAT TRANSFER ON TURBINE BLADES\*

Suhas V. Patankar and Rodney C. Schmidt  
University of Minnesota  
Minneapolis, Minnesota

A modified form of the Lam-Bremhorst low-Reynolds-number  $k$ - $\epsilon$  turbulence model (ref. 1) has been developed for predicting transitional boundary layer flows under conditions characteristic of gas turbine blades. Since previously reported work (refs. 2,3) has outlined the basic form of the model and its application to zero-pressure gradient flows with free-stream turbulence, this paper will primarily describe the application of the model to flows with pressure gradients, and will include tests against a number of turbine blade cascade data sets. Also, some additional refinements of the model made in recent months will be explained.

### INTRODUCTION

The difficulty, and yet great importance, of accurately predicting external heat transfer on gas turbine blades has stimulated a large amount of research dedicated to understanding and modeling transitional boundary layer flows. The primary factors found to influence this phenomenon include Reynolds number, free-stream turbulence, pressure gradients and streamline curvature, all of which are present on a typical gas turbine blade. Although many approaches can and have been taken in modeling this process, our work has focused on exploring and developing the potential of low-Reynolds-number (hereafter abbreviated as "LRN") forms of the  $k$ - $\epsilon$  turbulence model for solving this type of problem.

A variety of different LRN modifications have been proposed in the literature for the purpose of extending the validity of two equation turbulence models through the viscous sublayer to the wall (see for example reference 4 for a good review). One attractive characteristic of this type of model is the seemingly natural process by which boundary layer transition from laminar to turbulent flow is simulated without requiring a separate model. However, although some of these models had already been used to predict heat transfer on gas turbine blade cascades prior to the initiation of our work (refs. 5,6,7), little had been reported documenting predictive capabilities for the less complex case of flat plate flow. As a result, our previously reported work began by evaluating two relatively popular LRN models with respect to the prediction of transition on flat plates under the influence of free-stream turbulence. This work showed that although these models do predict the qualitative aspects of transition correctly, the starting location and length over which it occurs is generally not well predicted.

---

\*Work done under NASA Grant NAG-3-579

Subsequent to this evaluation a simple modification was proposed which could be applied within the framework of a LRN  $k$ - $\epsilon$  turbulence model, and which was designed to improve the prediction of boundary layer transition without affecting the fully turbulent model. The calibration of this model and application to flat plate zero pressure gradient flows, also reported earlier, proved to be fairly successful. Thus, this work has been pursued and the purpose of this paper is to report on the application of the model to predict experimental results of transitional flows with both free-stream turbulence and pressure gradients, and also to actual turbine blade cascade experiments.

## NOMENCLATURE AND SYMBOLS

$A, B$	Empirical parameters in the proposed modification. Correlated as functions of $Tu_e$
$C_\mu, C_{\epsilon 1}, C_{\epsilon 2}$	Constants in the two-equation turbulence models.
$f_\mu, f_1, f_2$	Low-Reynolds-number functions.
$h, h'$	Mean and fluctuating static enthalpy
$H$	Total enthalpy
$k$	Turbulent kinetic energy
$K$	Acceleration parameter $K = \nu/U^2 (\partial U/\partial x)$
$L$	Turbulence length scale $L = k^{1.5}/\epsilon$
$P$	Static pressure
$P_k$	Production term in the modeled $k$ equation
$Pr$	Molecular and Turbulent Prandtl numbers
$Re_\theta$	Reynolds number based on momentum thickness
$Re_{\theta, s}$	Momentum thickness Reynolds numbers at the start of transition
$R_t$	Turbulence Reynolds number $R_t = k^2/(\nu\epsilon)$
$R_y$	Wall Coordinate Turbulence Reynolds number $R_y = k \cdot 5y/\nu$
$St$	Stanton number
$Tu$	Turbulence intensity, $Tu = \{1/3(\overline{u'^2} + \overline{v'^2} + \overline{w'^2})\}^{.5}/U$
$U$	Mean velocity in the $x$ direction
$u', v', w'$	Fluctuating velocities in the $x, y, z$ directions
$x$	Streamwise direction coordinate
$y$	Cross-stream coordinate
$\rho$	Fluid density
$\delta$	Boundary layer thickness
$\theta$	Momentum thickness of the boundary layer
$\Lambda$	Acceleration parameter $\Lambda = \delta^2(dU/dx)/\nu$
$\epsilon$	Dissipation rate
$\mu$	Molecular viscosity
$\mu_t$	Eddy or turbulent viscosity
$\nu$	Kinematic viscosity, $\nu = \mu/\rho$
$\sigma_k, \sigma_\epsilon$	Empirical constants in the turbulence models.

### Subscripts

$c$	denoting critical
$e$	denoting free-stream value
$0$	denoting value at $x=0$

## BASIC EQUATIONS AND THE TURBULENCE MODEL

For the results presented in this work, the following forms of the time averaged continuity, momentum, and energy equations were solved.

$$\partial(\rho U)/\partial x + \partial(\rho V)/\partial y = 0 \quad (1)$$

$$\rho U[\partial U/\partial x] + \rho V[\partial U/\partial y] = \partial/\partial y[\mu \partial U/\partial y - \rho \overline{u'v'}] - dP/dx \quad (2)$$

$$\rho U[\partial H/\partial x] + \rho V[\partial H/\partial y] = \partial/\partial y[(\mu/Pr)\partial H/\partial y - \rho \overline{h'v'}] + \partial/\partial y \left\{ U[(1-1/Pr)\mu \partial U/\partial y - \rho \overline{u'v'}] \right\} \quad (3)$$

where  $H=h+U^2/2$ . Also the fluid is assumed to be a perfect gas with constant specific heat. A LRN form of the  $k$ - $\epsilon$  turbulence model is used to determine the turbulent shear stress and turbulent heat flux by defining

$$-\rho \overline{u'v'} = \mu_t (\partial U/\partial y) \quad (4)$$

$$-\rho \overline{h'v'} = (\mu_t/Pr_t)\partial h/\partial y, \quad \text{with } Pr_t = 0.9 \quad (5)$$

and by solving the following two additional transport equations for  $k$  and  $\epsilon$ .

$$\rho U[\partial k/\partial x] + \rho V[\partial k/\partial y] = \partial/\partial y[(\mu + \mu_t/\sigma_k)\partial k/\partial y] + \mu_t(\partial U/\partial y)^2 - \rho \epsilon \quad (6)$$

$$\rho U[\partial \epsilon/\partial x] + \rho V[\partial \epsilon/\partial y] = \partial/\partial y[(\mu + \mu_t/\sigma_\epsilon)\partial \epsilon/\partial y] + C_{\epsilon 1} f_1 (\epsilon/k) \mu_t (\partial U/\partial y)^2 \quad (7)$$

$$\text{where} \quad \mu_t = \rho C_\mu f_\mu (k^2/\epsilon) \quad (8)$$

The constants  $C_\mu$ ,  $C_{\epsilon 1}$ ,  $C_{\epsilon 2}$ ,  $\sigma_k$ , and  $\sigma_\epsilon$ , and the LRN functions  $f_1$ ,  $f_2$  are given in reference 8. The function  $f_\mu$  has been slightly changed as compared to the Lam-Bremhorst form to improve the predictions at very low  $Tu$ . Previous work had shown that the Lam-Bremhorst model did not predict transition for free-stream turbulence levels of lower than about 1% (refs. 2,7). Our investigation showed that this was due to the particular two parameter correlation for  $f_\mu$  ( $f_{\mu, LB} = f_\mu[R_t, R_y]$ ) chosen by Lam and Bremhorst which, under certain conditions predicted  $f_\mu \gg 1$ . Since the function  $f_\mu$  is intended to vary only from 0 to 1, this problem could be eliminated by simply restricting the magnitude of  $f_\mu$ . The details of this are given in reference 8. For the calculations given here,  $f_\mu$  was calculated as

$$f_\mu = \min(1., .5 + .0025 * R_t, f_{\mu, LB}) \quad (9)$$

The modification introduced to improve boundary layer transition predictions affects the so-called production term in the  $k$  equation,  $P_k = \mu_t (\partial U/\partial y)^2$ . (Note that the use of the words "production term" has been used rather loosely here to refer only to the quantity in the model, not a term in the exact form of the  $k$  equation.) This is done by limiting the magnitude of  $P_k$  before a specified stability limit ( $R_{\theta, C} = 125$ ), and then limiting the growth rate of  $P_k$  afterward. The details and the numerical implementation of this is given in reference 8. However, the basic relationship can be expressed as follows;

$$[\partial P_k / \partial t]_{\max} = A * P_k + B \quad (10)$$

The functions  $A$  and  $B$  have been correlated to the free-stream turbulence such that under flat-plate conditions the model predicts transition occurring at momentum thickness Reynolds numbers at the beginning and end of transition in accordance with the correlation of Abu-Ghannam and Shaw (ref. 9). It should be realized that the behavior shown in Figure 1 is unique to the LRN functions used in this model. Somewhat different values must be used with, for example, the Jones Launder model (ref. 10) to achieve similar results (see ref. 8). It also reflects somewhat different values than reported earlier in reference 2. This is a result of a reevaluation in the high  $Tu$  range, and also to the minor modification made to the  $f_\mu$  function given in eq. (9).

## COMPUTATIONAL PROCEDURE

Although details cannot be given here, a brief overview of some of the practical aspects of the computational procedure is appropriate. Before one can begin any computation, starting profiles and boundary conditions must be specified such that the actual problem of interest is solved. For a two equation turbulence model, this must include values for  $k$  and  $\epsilon$  in addition to the velocity and enthalpy. For all of the results presented here the following procedure was followed.

**Initial Starting Location:** The method of Thwaites ( see ref. 11, pg 315 ) was used to compute the momentum thickness Reynolds number variation from either the leading edge or the stagnation point. All calculations were then started at a streamwise location such that the momentum thickness Reynolds number was less than about 25. Our previous work showed that this minimized sensitivity to variations in initial profiles (ref. 2).

**Velocity:** Following the procedure of Rodi and Scheuerer (refs. 6,7), a Pohlhausen polynomial representation of the velocity profile was used. This requires an approximation for the local boundary layer thickness  $\delta$ , and an acceleration parameter  $\Lambda = \delta^2 U' / \nu$ . The details of this are given in reference 8. The local free-stream velocity and velocity gradient was determined from the experimental conditions.

**Enthalpy:** The total enthalpy in the free-stream was assumed to remain constant for all cases considered. For flat plate flows the starting enthalpy profile was derived from an approximate temperature-velocity profile relationship as per reference 6. For the turbine blade calculations, which were started near a stagnation point, this procedure was slightly modified to allow the thermal boundary layer  $\delta_T$ , to be different than the velocity boundary layer. This was controlled by estimating the stagnation point heat transfer coefficient and relating this to  $\delta_T$ . The details are given in reference 8.

**$k$  and  $\epsilon$ :** The free-stream values of  $k$  and  $\epsilon$  were found by relating them to the experimentally reported values of the free-stream turbulence intensity. For isotropic turbulence, this implies that

$$k_e = 1.5(Tu_e U_e)^2 \quad (11)$$

The value of  $\epsilon$  must be found such that the calculated decay in  $k$  with distance matches the data when the following two ordinary differential equations are solved.

$$U_e(dk_e/dx) = -\epsilon_e \quad (12)$$

$$U_e(d\epsilon_e/dx) = -C_{\epsilon 2} (\epsilon_e^2/k_e) \quad (13)$$

Documentation of these values for each case studied and the comparison with the experimental data is provided in reference 8. Since our previous work had shown the value of specifying  $k_e$  based on  $u'$  only, when possible this was always done.

When the experimental data is not sufficient to determine the dissipation length scale, such as is the case with much of the turbine blade cascade data, the calculations assume a small value of  $\epsilon$  such that  $k$  remains essentially constant. Note that because of the relationship between  $k$  and  $Tu$  expressed in eq. (10), even if the value of  $k$  remains constant,  $Tu$  will vary with free-stream velocity.

For convenience, the initial profile specification of  $k$  and  $\epsilon$  is similar to that of Rodi and Scheuerer (ref. 7) except that their parameter " $a_1$ " was always assumed equal to unity. Details of this are also given in reference 8.

### COMPARISON OF THE COMPUTATIONS TO EXPERIMENTS WITH FAVORABLE PRESSURE GRADIENTS

Taken together, the data sets of Blair (refs. 12,13), and of Rued and Wittig(refs. 14,15,16) provide a good variety of well documented experiments where the effects of both acceleration and free-stream turbulence on transition are represented. Both sets of data also provide the experimentally determined variation of  $Tu$  over the test sections, a key requirement for accurately modeling the transition process. Furthermore, the experiments of Rued have the additional attractive characteristic of representing wall to gas temperature ratios that are similar to those experienced on a gas turbine blade.

The experiments of Blair were set up so as to provide a flow with essentially constant acceleration, and two such levels of acceleration were explored. The magnitude of the acceleration parameter  $K$  corresponded to  $0.2 \times 10^{-6}$ , and  $.75 \times 10^{-6}$ . In figure 2, the Stanton number data found for the lowest acceleration case is shown for three different turbulence generating grids and compared to the computations. Although the Stanton number in the fully turbulent region is under-predicted, the location and extent of transition is reproduced fairly well. In Figure 3, results for the higher acceleration are shown. Here, the location of transition is reasonably reproduced at the higher turbulence level, but deviates somewhat in the lower turbulence case. Compared to the calculation, the experiments show the onset of transition to be further downstream, and the extent of the transition region to be longer. Furthermore, the extent to which the fully turbulent Stanton number is underpredicted has increased. The effect on transition is not unexpected, as we know that acceleration has a stabilizing effect on turbulence. However, it is not clear why the fully turbulent predictions were low. In our opinion, the most likely possibilities are an inadequate modeling of the turbulent heat flux (we used  $Pr_t = .9 = \text{constant}$ ), and/or a problem in the dissipation equation in the near wall region during acceleration.

Figure 4 shows the variation over the test section of the acceleration parameter  $K$  for three of the test cases reported by Rued. Note that these achieve significantly higher values of  $K$  than the tests of Blair. Figures 5-7 show a comparison of our calculations with the reported Stanton number data for these flows at four different levels of free-stream turbulence each. The model is quite successful at

predicting the heat transfer for cases 6 and 12, except in the initial region after the unheated starting length. One of the important observations made by Rued and Wittig (ref. 13) about their work, was that the results did not show a lower limit on  $Re_{\theta,S}$  of 163 as is used in the Correlation of Abu-Ghannam and Shaw for  $Tu > 7\%$ . This is reflected in these figures by our computations predicting the initial transition occurring too late at high  $Tu$ . For test case 10, grid two, the model indicates a relaminarization, whereas the experiments do not. Also, in grid 1, where transition occurs only after the acceleration has stopped, the transition length is underpredicted. In some ways this reminds us of the computation of Blair's data shown in figure 3, for grid 2.

## COMPARISON OF THE COMPUTATIONS WITH TURBINE BLADE CASCADE DATA

Figures 7-10 provide a comparison of the models predictions with the data provided by Daniels and Browne (ref. 17), and Hylton et al. (ref. 18). Data at two different Reynolds numbers is shown for each blade on both the suction and the pressure side.

Since the turbulence intensity measurements reported by Daniels and Browne were taken somewhat upstream of the test section, figures 7 and 8 show the results of computations assuming  $Tu_0 = 3.5\%$  and  $3\%$  for comparison purposes. As can be seen, the location and extent of transition, and the resulting heat transfer is very well predicted for these cases. The only significant variation between the data and the computation occurs at the higher Reynolds number in regions downstream of transition. On the suction side starting at  $S/L = 4.5$ , the flow experiences a region of adverse pressure gradient. Previous research has documented the failure of 2- $\epsilon$  LRN models such as that of Lam-Bremhorst to correctly calculate the near wall turbulence length scale in adverse pressure gradient flows, resulting in an over prediction of the skin friction and heat transfer (see ref. 19). For comparison, a computation is shown where the dissipation equation was modified in line with a suggestion of Launder (ref. 20) in the following manner.

$$C_{\epsilon 1} = 1.44 * \max(1, L/L_{\max})$$

where

$$L = k^{1.5} / \epsilon, \quad L_{\max} = 2.7y \quad (14)$$

The results of this additional modification show an improved prediction of the heat transfer on the suction side without influencing the transition predictions.

In figures 9 and 10, comparisons with the data of Hylton et al. are shown. These calculations show similar trends as was pointed out on the Daniels and Browne data, i.e., an excellent prediction of the lower Reynolds number data, but an over prediction of the heat transfer in the turbulent regions on both the suction and pressure sides for the higher Reynolds number case. Also, the modification given in eq. (14) is shown to reduce the predictions on the suction side down to match the data. However, there is a clear overshoot in the heat transfer predictions for run 145, which cannot be explained with reference to the dissipation equation correction. The reason for this difference may be related to the effects of curvature in the recovery region after the release of curvature. In the C3X blade the radius of curvature is small until about  $S/\text{arc} = .2$ .

## CONCLUSIONS

Tests of the transition model proposed against a wide range of flows with pressure gradient have shown that even without additional modifications, the model is quite satisfactory for predicting much of the data. However, it appears that the computations might be improved in the future by considering the following;

- (1) As the relationship between  $Re_{\theta}$  and  $Tu$  at high  $Tu$  is clarified experimentally, improvements could be incorporated into the correlations for  $A$  and  $B$ , and possibly  $Re_{\theta C}$ .
- (2) The length over which transition occurs during favorable pressure gradient conditions might be more accurately modeled by decreasing the value of  $A$  and/or  $B$  in some appropriate manner.
- (3) Improvements in the LRN functions relative to the fully turbulent flows with pressure gradients.
- (4) Appropriate incorporation of curvature effects into the transition modifications.

## REFERENCES

1. Lam, C. K. G., and Bremhorst, K., "A Modified Form of the  $k-\epsilon$  Model for predicting Wall Turbulence", *J. of Fluids Engineering*, Vol. 103, Sept. 1981, pp. 456-460
2. Schmidt, R. C., and Patankar, S. V., "Development of Low Reynolds Number Two Equation Turbulence Models for predicting External Heat Transfer on Turbine Blades" Proceedings of the 1986 Turbine Engine Hot section Technology Conference sponsored by the NASA Lewis Research Center, NASA Conference Publication 2444, Oct. 1986, pp. 219-232
3. Schmidt, R. C., and Patankar, S. V., "Prediction of Transition on a Flat Plate under the Influence of Free-Stream Turbulence using Low-Reynolds-Number Two-Equation Turbulence Models", ASME Paper 87-HT-32
4. Patel, V. C., Rodi, W., and Scheuerer, G., "A Review and Evaluation of Turbulence Models for Near Wall and Low Reynolds Number Flows", *AIAA Journal*, Vol. 23, 1985, p. 1308
5. Wang, J. H., Jen, H. F., and Hartel, E. O., "Airfoil Heat Transfer Using Low Reynolds Number Version of a Two Equation Turbulence Model.", *J. of Engineering for Gas Turbines and Power*, Vol. 107, No. 1, Jan. 1985, pp. 60-67
6. Rodi, W., and Scheuerer, G., "Calculation of Heat Transfer to Convection-Cooled Gas Turbine Blades", *J. of Engineering for Gas Turbines and Power*, Vol. 107, July 1985, pp. 620-627
7. Rodi, W., and Scheuerer, G., "Calculation of Laminar-Turbulent Boundary Layer Transition on Turbine Blades", AGARD-CPP-390
8. Schmidt, R. C. "Two-Equation Low-Reynolds-Number Turbulence Modeling of Transitional Boundary-Layer Flows Characteristic of Gas Turbine Blades", Ph. D. Thesis, Dept. of Mechanical Engineering, University of Minnesota, 1987
9. Abu-Ghannam, B. J., and Shaw, R., "Natural Transition of Boundary Layers -The Effects of Turbulence, Pressure Gradient, and Flow History", *J. of Mech. Eng. Science*, Vol. 22, No. 5, 1980, pp. 213-228
10. Jones, W. P., and Launder, B. E., "The Calculation of Low Reynolds Number Phenomena With a Two-Equation Model of Turbulence", *Int. J. of Heat and Mass Transfer*, Vol. 16, 1973, pp. 1119-113
11. White, F. M., Viscous Fluid Flow, McGraw-Hill, Inc. 1974

12. Blair, M. F., "Influence of Free-Stream Turbulence on Boundary Layer Transition in Favorable Pressure Gradients", ASME J. of Engineering for Power, Vol. 104, Oct. 1982, pp. 743-750
13. Blair, M. F., and Werle, M. J., "Combined Influence of Free-Stream Turbulence and Favorable Pressure Gradients on Boundary Layer Transition", UTRC Report R81-914388-17, Mar. 1981
14. Rued, K., and Wittig, S. "Free Stream Turbulence and Pressure Gradient Effects on Heat Transfer and Boundary Layer Development on Highly Cooled Surfaces", J. of Engineering for Gas Turbines and Power, Vol. 107, No. 1, Jan. 1985, pp. 54-59
15. Rued, K., and Wittig, S., "Laminar and Transitional Boundary Layer Structures in Accelerating Flow with Heat Transfer", ASME Paper No. 86-GT-97
16. Rued, K "Transitionale Grenzschichten unter dem Einfluss hoher Freistromturbulenz, intensiver Wandkuehlung und starken Druckgradienten in Heissgasstroemungen", Thesis submitted at the University of Karlsruhe, 1985
17. Daniels, L. D., Browne, W. B., "Calculation of Heat Transfer Rates to Gas Turbine Blades", Int. J. of Heat and Mass Transfer, Vol 24, No. 5, pp. 871-879, 1981
18. Hylton, L. D., Mihelc, M. S., Turner, E. R., Nealy, D. A., and York, R. E., "Analytical and Experimental Evaluation of the Heat Transfer Distribution Over the Surfaces of Turbine Vanes", NASA CR-168015, May 1983
19. Rodi, W., and Scheuerer, G., "Scrutinizing the k-ε Turbulence Model under Adverse Pressure Gradient Conditions", ASME J. of Fluids Eng., Vol 108, June 1986, pp 174-179
20. Launder, B. E., "Second Moment Closure: Methodology and Practice", Turbulence Models and Their Applications, Vol 2, Edition Eyrolles, Saint-Germain Paris, 1984

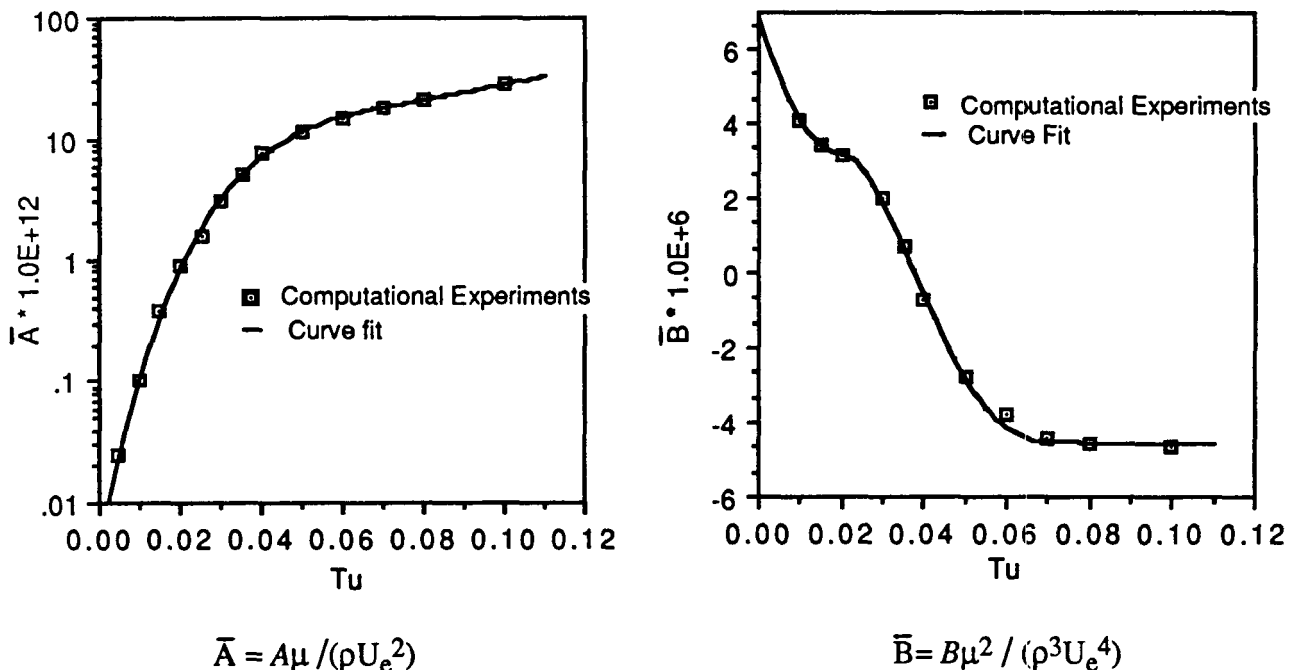


FIGURE 1 Variation in "A" and "B" with free-stream turbulence intensity



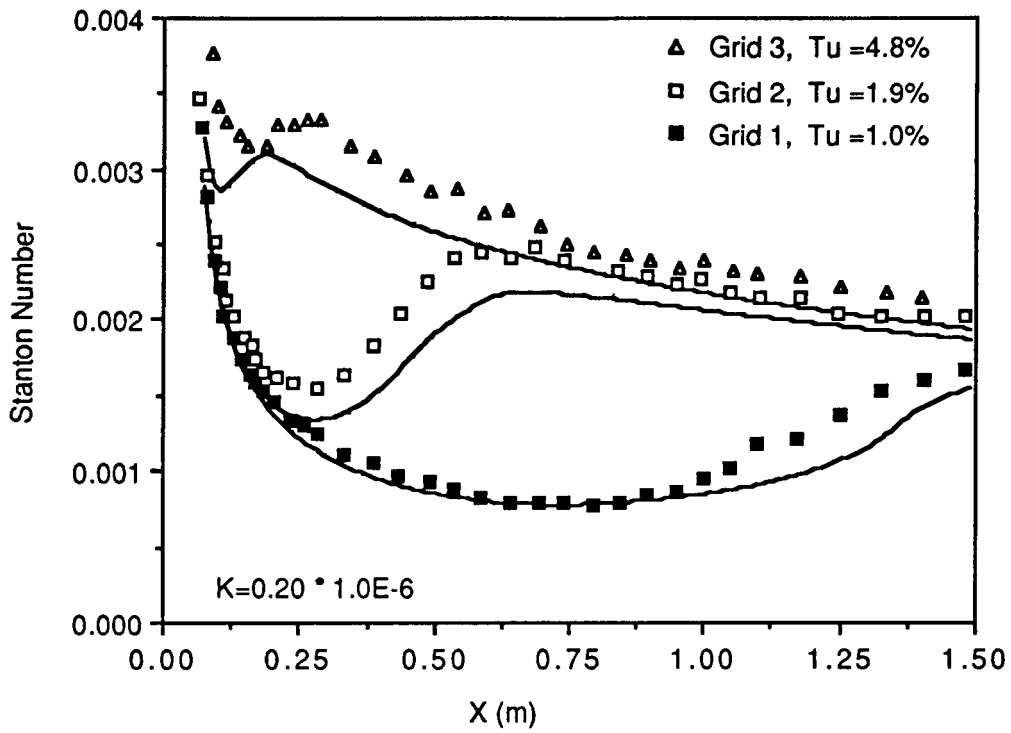


FIGURE 2 Comparison of the calculations with the lower acceleration test data of Blair

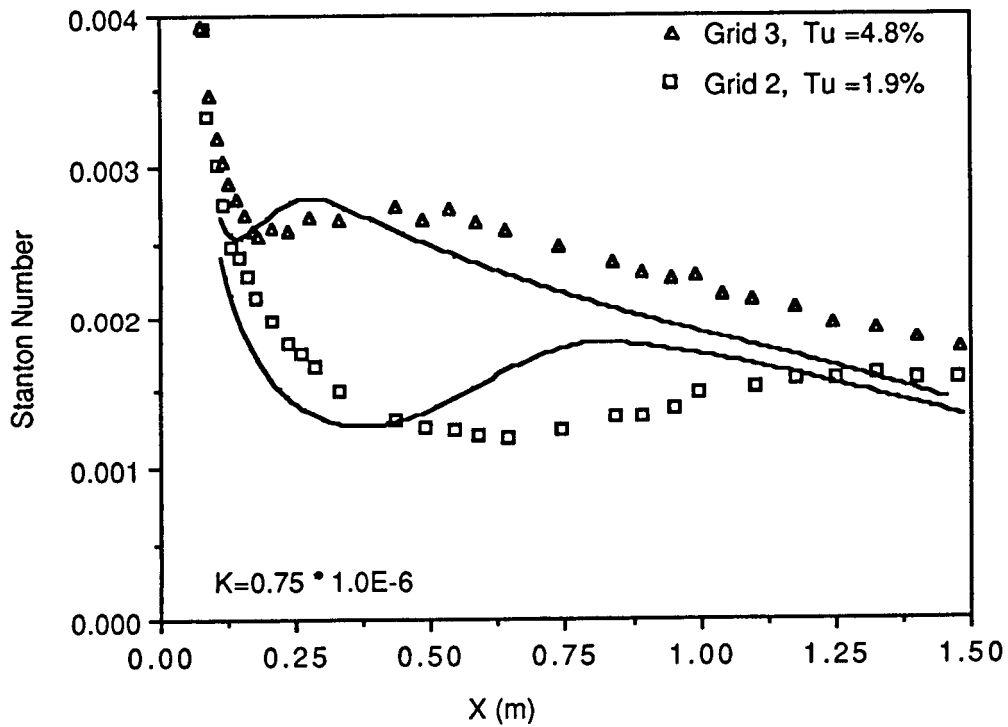


FIGURE 3 Comparison of the calculations with the higher acceleration test data of Blair

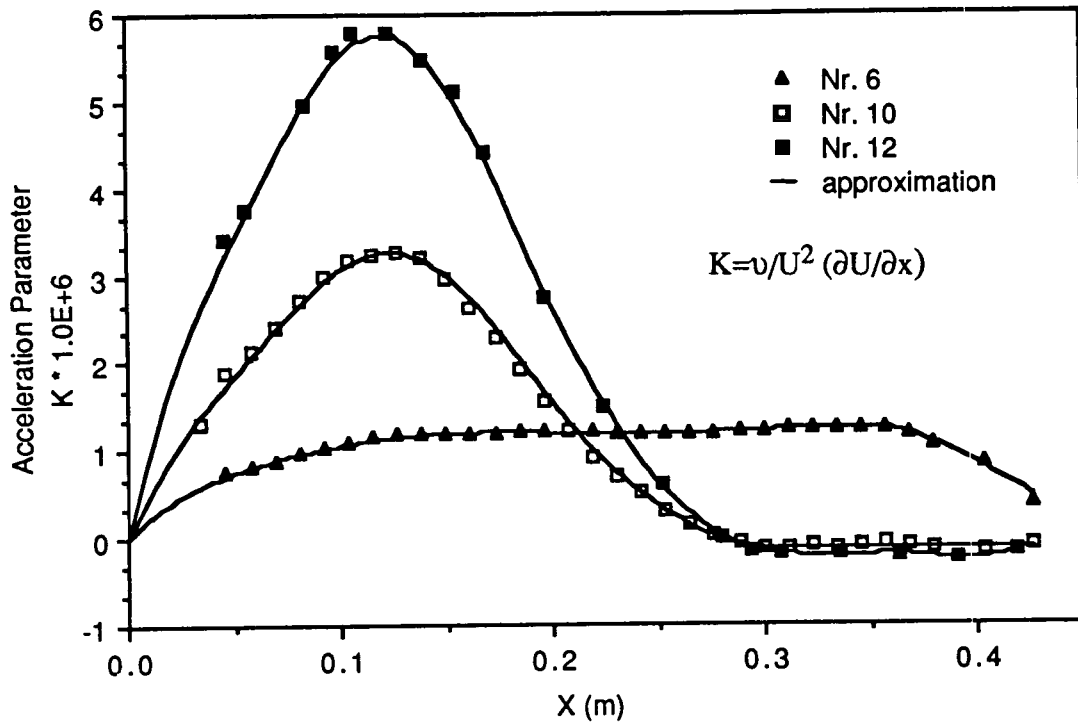


FIGURE 4 Variation in acceleration for three test cases of Rued

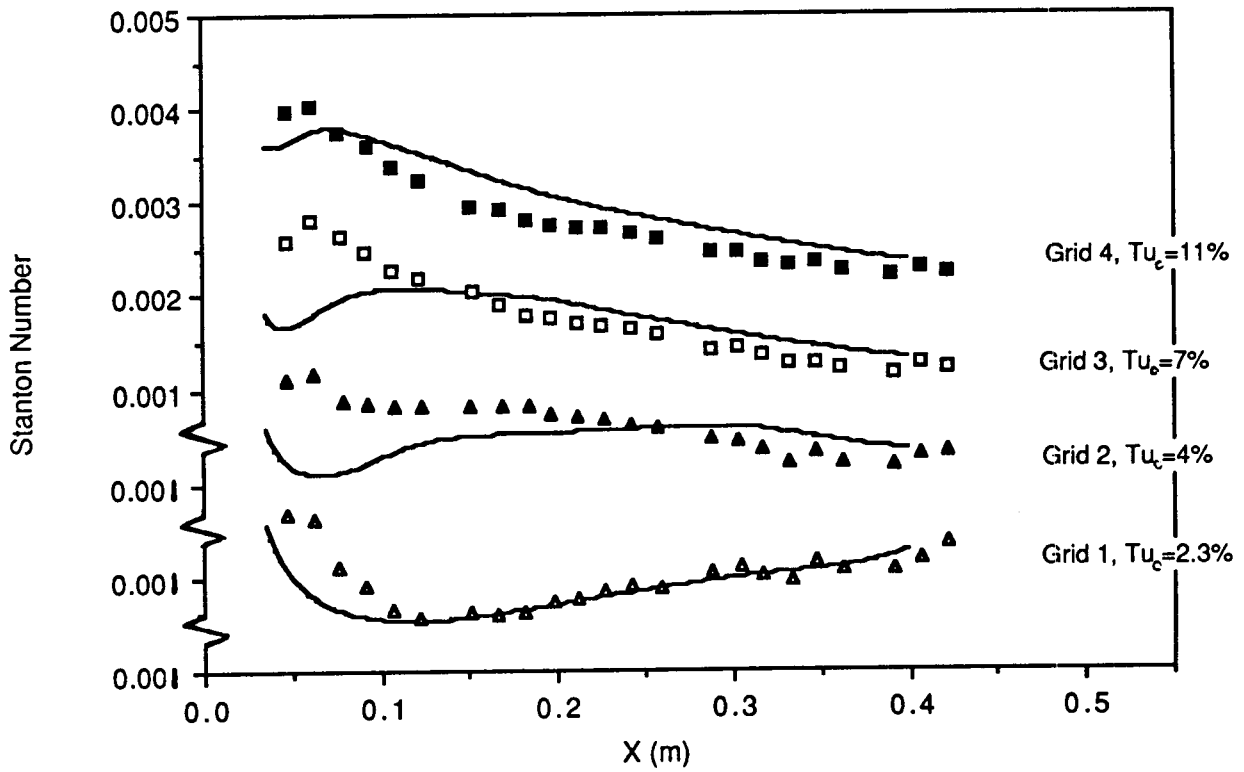


FIGURE 5 Comparison of the calculations with the data from case 6 of Rued

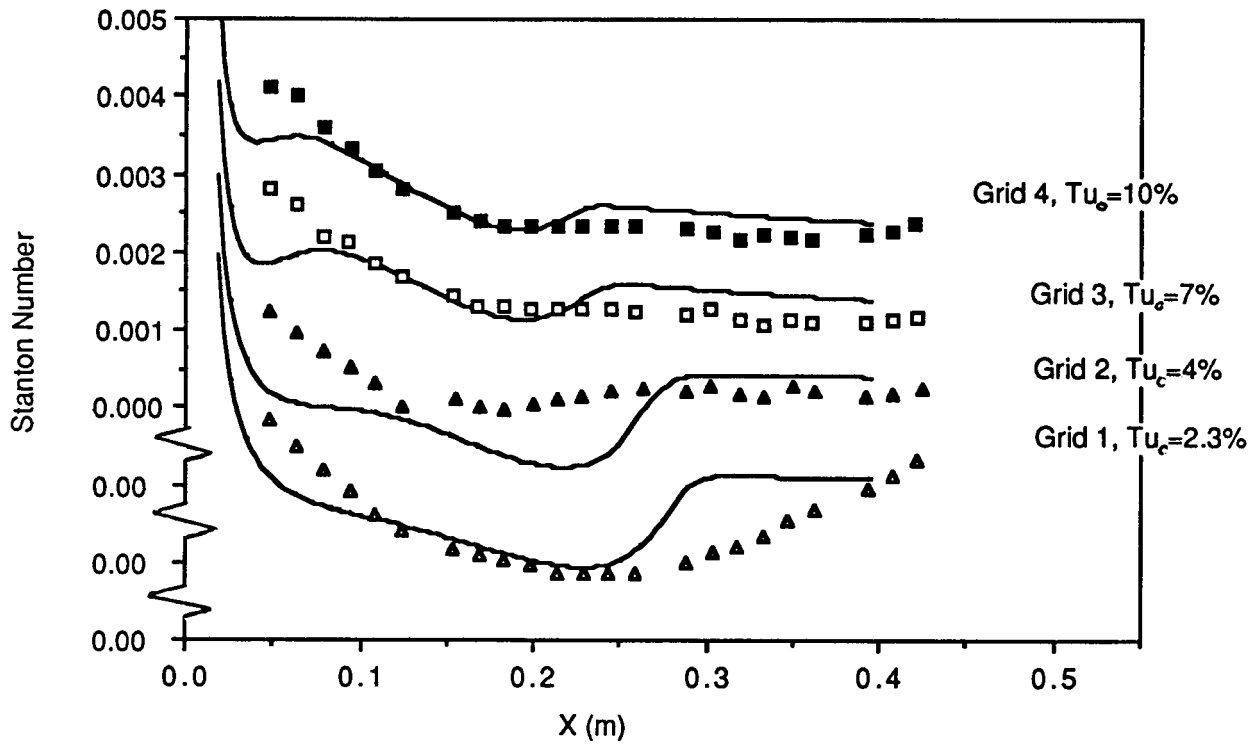


FIGURE 6 Comparison of the calculations with the data from case 10 of Rued

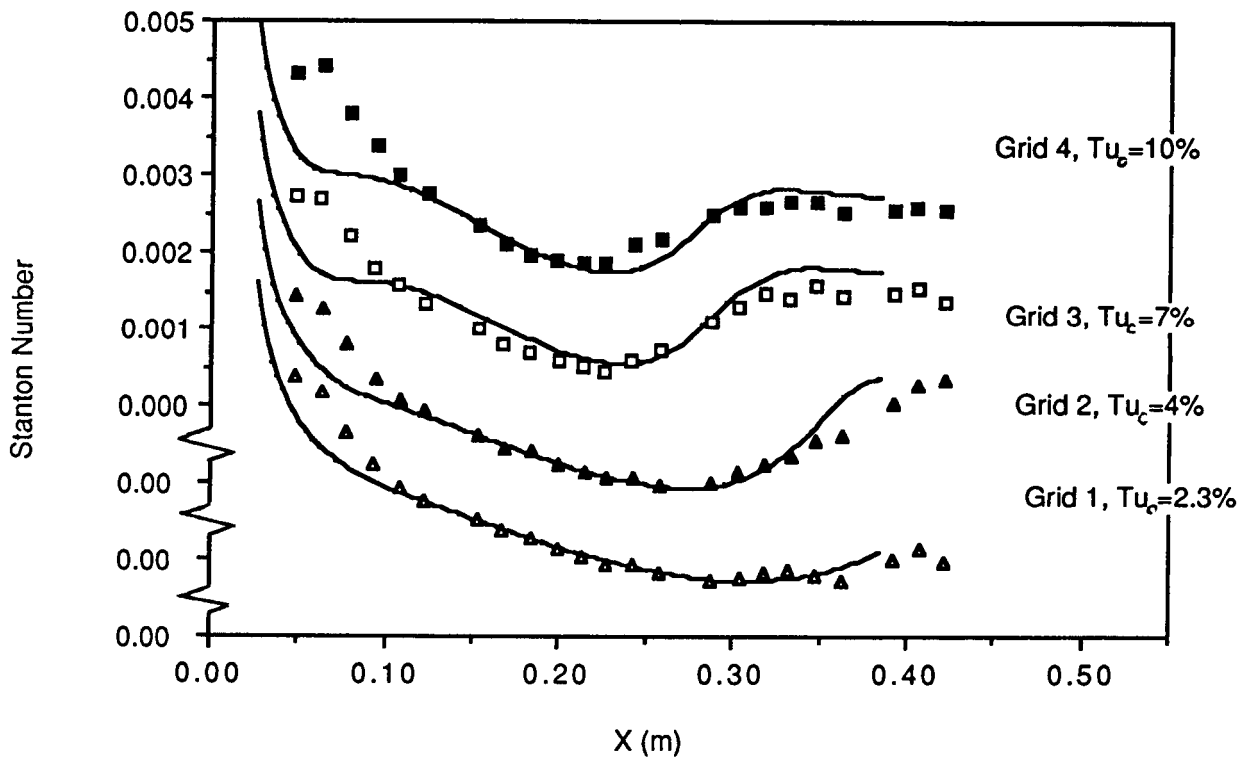


FIGURE 7 Comparison of the calculations with the data from case 12 of Rued

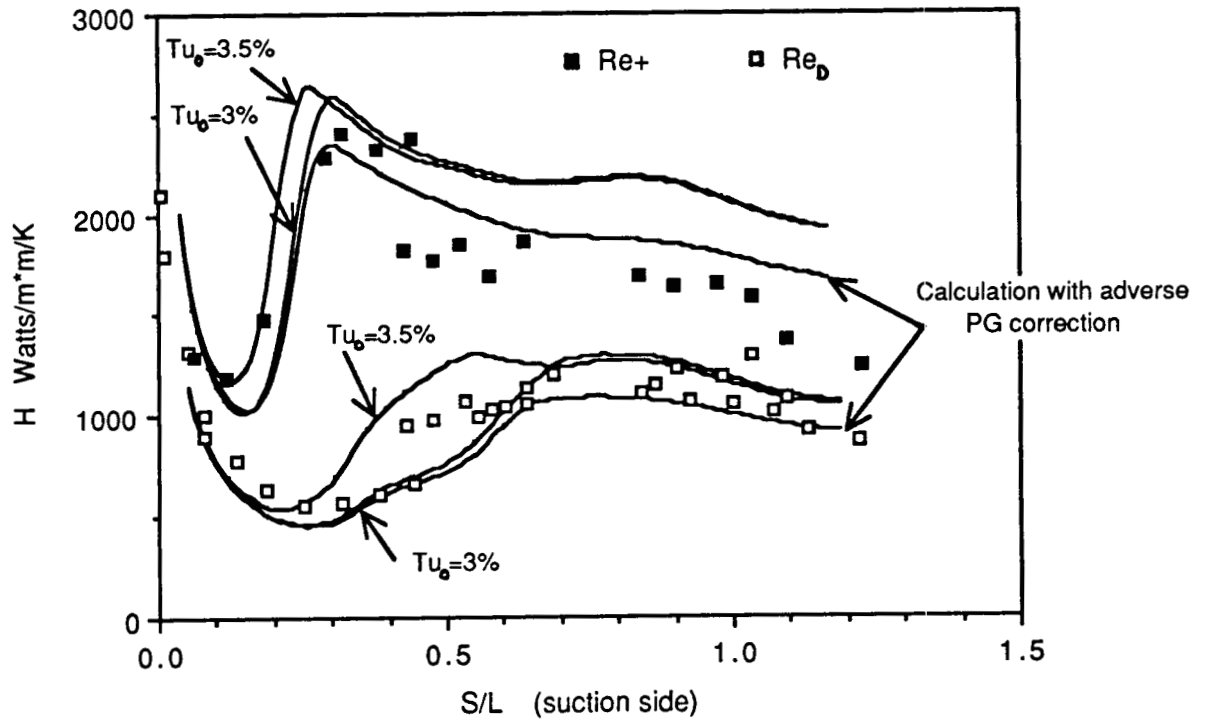


FIGURE 8 Comparison of the calculations with the data from Daniels and Browne on the suction side of the blade  $L=50.44$  mm

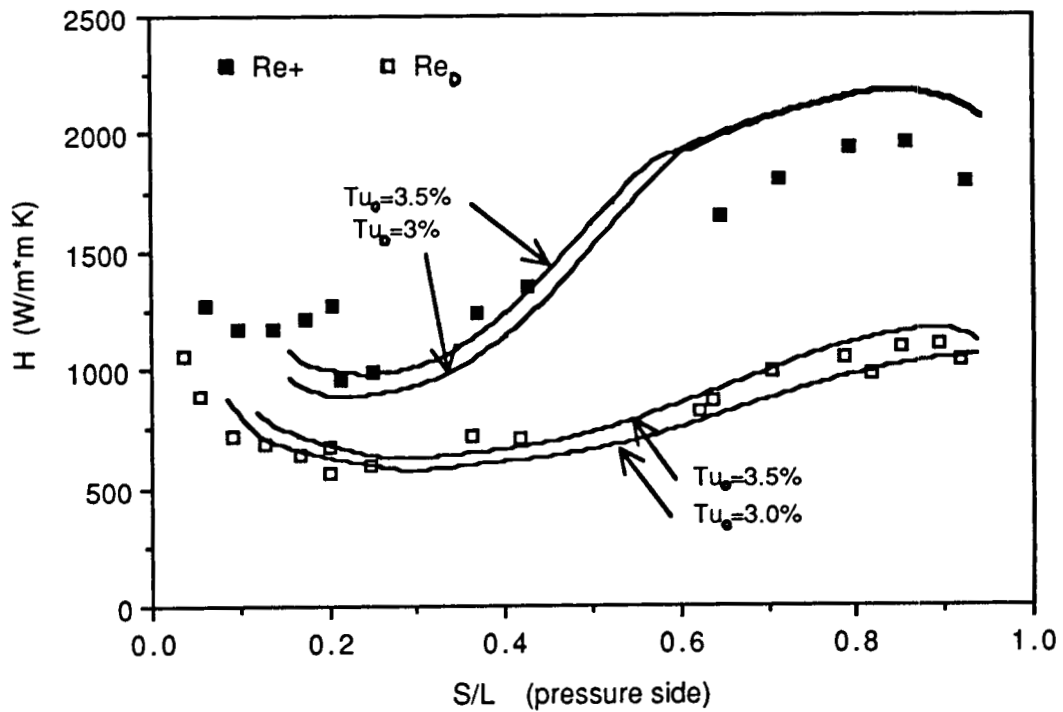


FIGURE 9 Comparison of the calculations with the data from Daniels and Browne on the pressure side of the blade  $L=50.44$  mm

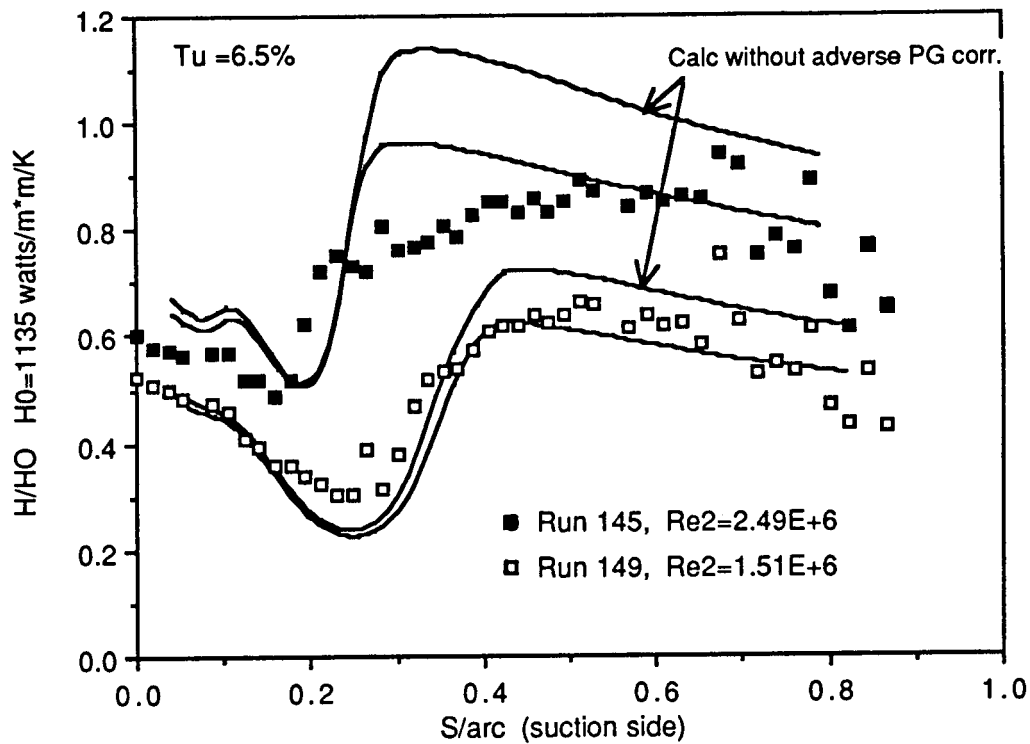


FIGURE 10 Comparison of the calculations with data on the suction side from runs 145 and 149 of the C3X blade of reference 18.  $\text{arc} = .18 \text{ m}$

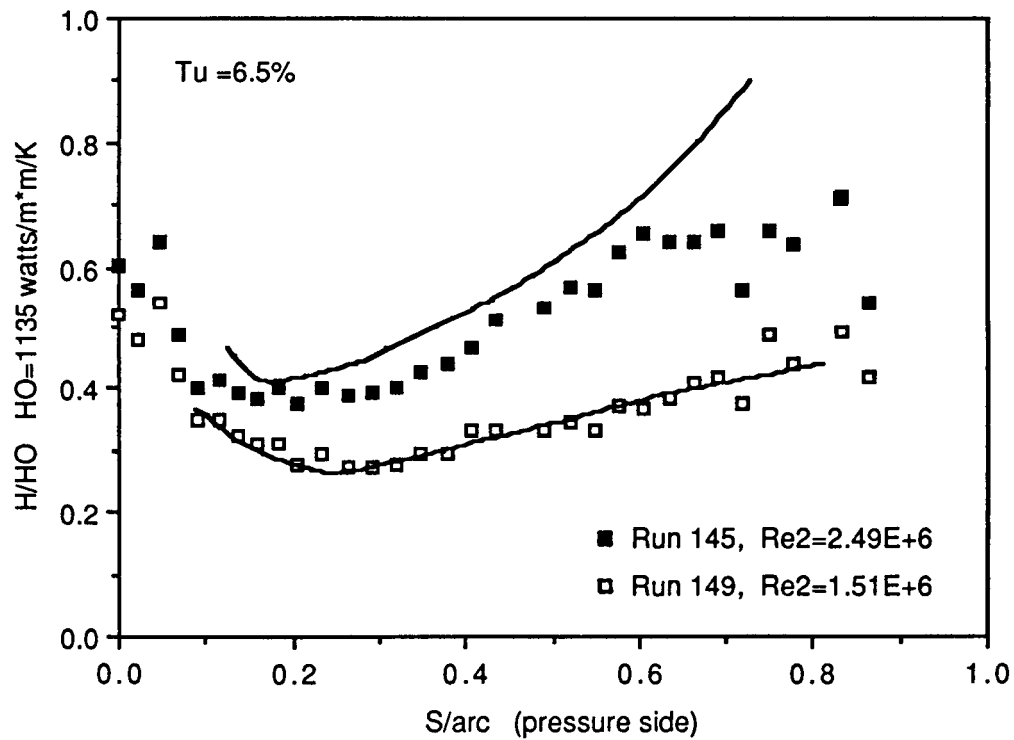


FIGURE 11 Comparison of the calculations with data on the pressure side from runs 145 and 149 of the C3X blade of reference 18.  $\text{arc} = .14 \text{ m}$